

## Single-molecule vibrational spectroscopy and microscopy: CO on Cu(001) and Cu(110)

L. J. Lauhon and W. Ho

Laboratory of Atomic and Solid State Physics and Cornell Center for Materials Research, Cornell University, Ithaca, New York 14853

(Received 6 May 1999)

Single-molecule vibrations of four isotopes of CO on Cu(001) and Cu(110) at 8 K have been measured by inelastic electron tunneling spectroscopy with the scanning tunneling microscope (STM-IETS). While the low energy hindered rotation exhibits strong intensity, the C-O stretch approaches the present detection limit of STM-IETS. By performing vibrational microscopy, the spatial distribution of the hindered rotation intensity is found to be more localized than the topographic depression in constant current images.

[S0163-1829(99)50336-6]

The vibrational spectrum of a molecule adsorbed on a solid surface can provide insight into the nature of the bonding and the local chemical environment. Vibrational spectroscopy can be performed using a variety of techniques including electron-energy-loss spectroscopy (EELS), infrared absorption spectroscopy (IRAS), Raman spectroscopy, inelastic neutron scattering, inelastic electron tunneling spectroscopy (IETS), and helium-atom scattering (HAS).<sup>1,2</sup> All of the aforementioned techniques rely on macroscopic numbers of molecules to achieve detectable signal levels. The signal is therefore an average over molecules whose local environments can vary due to defects, steps, and coadsorbates. With the development of the scanning tunneling microscope (STM), it was apparent that IETS might be performed on a single molecule in the junction of a STM,<sup>3,4</sup> thereby extending vibrational spectroscopy to the single-molecule limit and providing the STM with chemical sensitivity. One great advantage of performing vibrational spectroscopy with the STM is that the remarkable spatial resolution of STM images permits changes in molecular spectra to be correlated with variations in the local environment on an atomic scale.

It should be noted that in certain cases, the contribution of a single atom to the electronic spectrum measured with a STM can be deduced.<sup>5-8</sup> The STM is not generally capable of identifying adsorbates via electronic spectroscopy, however, due to the significant level broadening and shifting that occurs upon chemisorption. Vibrational energy levels, unlike electronic levels, retain sufficient molecular character to permit chemical identification.

The feasibility of single-molecule vibrational spectroscopy using a STM was demonstrated only recently.<sup>9</sup> A change in conductance as large as 12% was produced by exciting the C-H stretch vibration of an acetylene molecule on Cu(001). This represented an increase in sensitivity of at least  $10^9$  over other vibrational spectroscopies.<sup>10</sup>

In this paper, we report the observation of the C-O stretch and hindered rotation modes of single CO molecules adsorbed on Cu(001) and Cu(110) by STM-IETS. This observation represents an extension of STM-IETS to another functional group of great fundamental and practical interest. As the excitation mechanism is not well understood, the discovery of new tunneling-active modes is crucial to extending the applicability of STM-IETS and to developing a more mature theoretical understanding of the process.

A variety of surface analysis techniques have been used to study CO adsorbed on metal surfaces. CO adsorbs vertically on atop sites through the carbon atom on both Cu(001) and Cu(110) surfaces.<sup>11,12</sup> For CO on Cu(001), there are six vibrational modes: the C-O stretch ( $\nu_1$ ); the CO-Cu stretch ( $\nu_2$ ); the doubly degenerate hindered rotation ( $\nu_3$ ); the doubly degenerate hindered translation ( $\nu_4$ ).<sup>13</sup> The energies of these modes have been measured by EELS ( $\nu_{1-3}$ ),<sup>13,14</sup> IRAS ( $\nu_{1-3}$ ),<sup>15</sup> and HAS ( $\nu_4$ ).<sup>16</sup> The Cu(110) surface potential breaks the degeneracy of the  $\nu_3$  and  $\nu_4$  modes. This effect is weak, but splitting of the  $\nu_4$  mode has been inferred from electron stimulated desorption ion angular distribution studies.<sup>17</sup> EELS has been used to identify  $\nu_{1-4}$  on Ni(110) (Ref. 18) and Pd(110),<sup>19</sup> confirming the relative order in energy of the modes identified on copper by the techniques mentioned above.

Experiments were performed using a home-built variable temperature STM housed in an ultrahigh vacuum chamber with a base pressure of  $2 \times 10^{-11}$  Torr.<sup>20</sup> Sample and tip preparation have been described previously.<sup>9</sup> CO and its isotopes were dosed to coverages of  $\theta \sim 0.001$  at 8 K via a capillary array doser attached to a variable leak valve. Spectroscopic measurements were taken at 8 K with tips that, under typical imaging conditions of 1 nA and 0.25 V sample bias, imaged the CO as a round depression and did not resolve the copper substrate atoms. Tips were often modified by bringing them into contact with the surface, followed by field emission at  $\pm 10$  V. This procedure was found to produce tip configurations that were sharp and stable.

The STM implementation of IETS has been described previously in detail.<sup>9,20</sup> Briefly, the tip is positioned over the center of the CO molecule by locating the minimum in height using an iterative tracking routine. With the feedback off, the sample bias voltage is ramped over the range of vibrational peaks while a sinusoidal bias modulation is superimposed.<sup>21</sup> When the energy of the tunneling electrons is sufficient to excite a tunneling-active vibrational mode of the molecule, the conductance increases due to the onset of an inelastic tunneling channel. The derivative of the conductance exhibits a peak at the molecular vibrational energy  $\hbar\omega = eV_{\text{bias}}$ . The conductance  $\sigma = dI/dV$  and its derivative  $d\sigma/dV = d^2I/dV^2$  are proportional to the first and second harmonics of the tunneling current which are measured with a lock-in amplifier.  $I$ - $V$  curves were taken to determine the

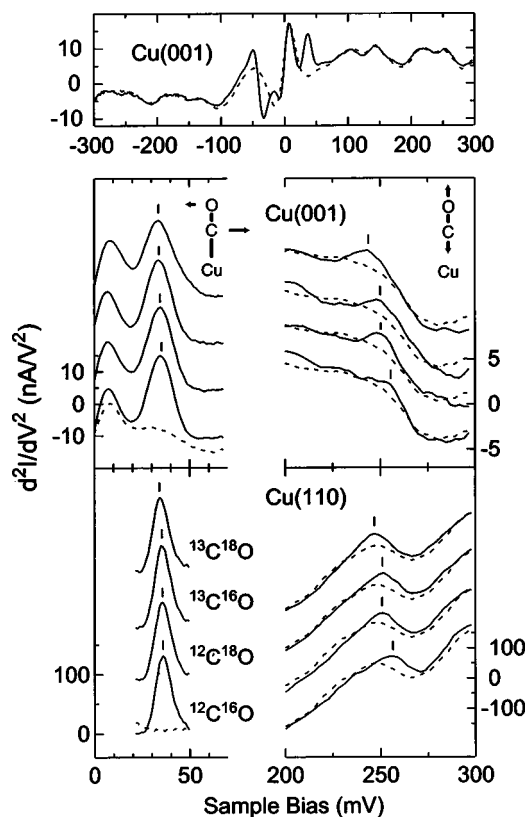


FIG. 1.  $d^2I/dV^2$  spectra taken over four CO isotopes at 8 K. Dashed lines are background spectra taken over clean areas of the surface. Single atom tracking was automatically performed every  $\sim 150$  sec to maintain the relative positions of the tip and molecule. The uppermost graph shows a typical spectrum for the  $^{12}\text{C}^{16}\text{O}$  signal averaged over 8 h with a 7 mV bias modulation and a gap resistance of 250 M $\Omega$  (1 nA at 0.25 V). The lower graphs display regions of the energy spectrum where the CO hindered rotation and C-O stretch modes, indicated schematically, are observed. Isotope ordering is consistent with labels in lower left. Low- and high-energy spectra were taken with 1 mV and 2.5 mV dc bias increments and 10 min and 50 min signal averaging times, respectively. Cu(001) spectra were taken with a gap resistance of 250 M $\Omega$  (1 nA at 0.25 V) and a bias modulation of 7 mV. For Cu(110), low-energy spectra were taken with a 10 M $\Omega$  (10 nA at 0.1 V) gap resistance and a 2 mV bias modulation, while high-energy spectra were taken with a 25 M $\Omega$  (10 nA at 0.25 V) gap resistance and a 7 mV bias modulation. The 2 mV modulation spectra were taken over the bias range shown. Lines above peaks serve as guides to the eye.

proportionality constants. For comparison, background spectra were taken over clean areas of the surface.

Inelastic tunneling spectra for  $^{12}\text{C}^{16}\text{O}$ ,  $^{12}\text{C}^{18}\text{O}$ ,  $^{13}\text{C}^{16}\text{O}$ , and  $^{13}\text{C}^{18}\text{O}$  on Cu(001) and Cu(110) are shown in Fig. 1 for the energy ranges in which the C-O stretch and hindered rotation modes are observed. Background spectra are shown for comparison. The peaks in the lower energy region for the four isotopes are easily observed. Peaks in the C-O stretch region are discerned by comparison with the background spectrum; the shift of spectral weight due to isotopic variation is clearly visible. In general, the background structure varied depending on the state of the tip, but the CO vibrational peaks were always observed for reasonably sharp tips. Peak positions were determined by fitting the spectrum taken over the molecule to a Gaussian and a polynomial simulta-

TABLE I. Summary of vibrational energies in meV for CO on Cu observed by STM-IETS compared to those from IRAS. The values in parentheses are vibrational energies from negative voltage scans. Uncertainties in STM-IETS values are  $\pm 1$  meV for the CO stretch ( $\nu_1$ ) and  $\pm 0.3$  meV for the hindered rotation ( $\nu_3$ ). Displacements associated with  $\nu_1$  and  $\nu_3$  are sketched in Fig. 1.

Mode	Surf.	Method	$^{12}\text{C}^{16}\text{O}$	$^{12}\text{C}^{18}\text{O}$	$^{13}\text{C}^{16}\text{O}$	$^{13}\text{C}^{18}\text{O}$
$\nu_3$	(001)	STM-IETS	36.3(33.2)	36.1	35.4	35.2
$\nu_3$	(001)	IRAS <sup>a</sup>	35.6	35.3	34.5	34.2
$\nu_1$	(001)	STM-IETS	256(256)	251	251	244
$\nu_1$	(001)	IRAS <sup>a</sup>	258			
$\nu_3$	(110)	STM-IETS	36.3	36.0	35.4	35.0
$\nu_1$	(110)	STM-IETS	257(257)	251	252	246
$\nu_1$	(110)	IRAS <sup>b</sup>	259	252		

<sup>a</sup>Reference 15.

<sup>b</sup>Reference 31.

neously. The initial polynomial coefficients were determined by fitting a background spectrum taken over the clean surface. A summary of the identified peak energies based on multiple observations with different tips and molecules is shown in Table I. Peak energies determined by IRAS are also shown for comparison. Based on the observed isotopic shifts and comparisons with previous studies, the 36 meV peak is identified as the CO hindered rotation and the 256 meV peak as the C-O stretch. The positions of the C-O stretch for Cu(001) and Cu(110) as measured by STM-IETS are in agreement with IRAS measurements (Table I). They also match the IETS value of 256.5 meV for the presumed linear species of CO on Ni particles on alumina.<sup>22</sup> The CO hindered translation at 4 meV (Ref. 16) and the CO-Cu stretch at 42 meV (Ref. 15) were not observed by STM-IETS.

The C-O stretch energy at negative bias was not measurably different from the positive bias value, but this does not preclude the existence of a Stark shift. For the C-O stretch on Cu(001),  $dv/dE \sim 10$  meV/V- $\text{\AA}^{-1}$  (Ref. 23). Assuming planar electrodes and a tunneling gap of 5  $\text{\AA}$ , the energy difference between the negative and positive bias C-O stretch peaks should be approximately 1 meV. The error in the C-O stretch position is comparable to the expected Stark shift. The position of the positive bias CO hindered rotation measured by STM-IETS is higher than the IRAS value. The magnitude of the peak positions at negative bias for all isotopes were on average 3 meV lower than those at positive bias. If this shift were due to the Stark effect, the approximations above suggest that  $dv/dE \sim 200$  meV/V- $\text{\AA}^{-1}$ . This is an order of magnitude greater than theoretical estimates.<sup>24</sup> As an experimental check, the tip was moved away from the surface and the peak position of the hindered rotation was measured every 0.5  $\text{\AA}$  over a total distance of 3  $\text{\AA}$  by decreasing the tunneling current set point. No monotonic change in the peak position was observed, in contrast to the 0.5 meV shift expected from the estimated  $dv/dE$ . The asymmetry in the line shape of the hindered rotation mode at positive and negative biases may be due to interactions between the adsorbate and substrate.

The relative change in conductance,  $\Delta\sigma/\sigma$ , is directly related to the fraction of electrons that can tunnel inelastically

and is thus a convenient quantity for comparing the relative cross sections of the tunneling-active modes. The  $\Delta\sigma/\sigma$  is determined by integrating  $d\sigma/dV$  over the peak region and normalizing by  $\sigma$  on the low-energy side of the peak. For CO on Cu(001) at a 250 M $\Omega$  gap resistance, the largest observed  $\Delta\sigma/\sigma$  was 8% for the hindered rotation and 1.5% for the C-O stretch. With the same tip and gap resistance,  $\Delta\sigma/\sigma$  for the C-H stretch mode of acetylene on Cu(001) was 15%. The magnitude of  $\Delta\sigma/\sigma$  due to the C-O stretch is in agreement with an early calculation based on the dipole scattering approximation,<sup>25</sup> but the large  $\Delta\sigma/\sigma$  of the hindered rotation suggests that this theory is at best an incomplete description of inelastic tunneling processes. Other theories of STM-IETS based on resonance scattering<sup>26,27</sup> predict larger values of  $\Delta\sigma/\sigma$ , but disagree as to the sign. Scattering theories for more well established techniques such as EELS and IRAS rely on wave-vector-dependent selection rules to explain the observed peak intensities.<sup>1</sup> The tunneling-active modes observed to date do not suggest a comparable set of selection rules for STM-IETS.

The magnitude of the C-O stretch peak at negative bias was on average a factor of 2 lower than at positive bias. The same effect has been seen in macroscopic IETS and attributed to the difference in tunneling probabilities for electrons that tunnel before or after losing energy to the molecular vibration.<sup>28</sup> The hindered rotation at negative bias was not measurably weaker than at positive bias. This is consistent with the simple picture given above as the energy difference between tunneling electrons at negative and positive biases is much smaller for the hindered rotation.

The full width at half maximum (FWHM) for the peaks in Fig. 1 taken with a 7 mV bias modulation is  $13 \pm 1$  meV. The FWHM for the hindered rotation on Cu(110), taken with a 2 mV bias modulation, is  $9.5 \pm 0.5$  meV. For a given temperature and bias modulation, the FWHM variation between different STM tips was  $\sim 2$  meV. The FWHM of the hindered rotation on Cu(001) was measured for bias modulations of 2-15 mV. By extrapolating to zero bias modulation at 8 K, a peak width of  $9 \pm 1$  meV was found. By extrapolating to 0 K from measurements at and above 8 K, the intrinsic width was estimated to be  $6 \pm 2$  meV. Details will be reported elsewhere.<sup>29</sup>

The CO-Cu stretch mode at 42 meV was not observed due to a small inelastic tunneling cross section as well as the proximity of the hindered rotation at 36 meV; the 6 meV separation between the two modes is comparable to the energy resolution determined by the intrinsic width. The assignment of the hindered translation mode at 4 meV is complicated by two factors. First, the separation between the positive and negative bias peaks is comparable to the energy resolution at 8 K. Additionally, coupling between substrate excitations, including phonons, and the hindered translation may lead to asymmetries in the line shapes. A small positive peak at  $\sim 5$  meV and a corresponding dip at negative bias were consistently observed and may be due to excitation of the hindered translation mode.

Figures 2(a) and 2(b) show constant current and vibrational microscopy images taken concurrently at the bias corresponding to the hindered rotation energy. At each point, the tip position was recorded with the feedback on to produce the topograph of Fig. 2(a). The feedback was then

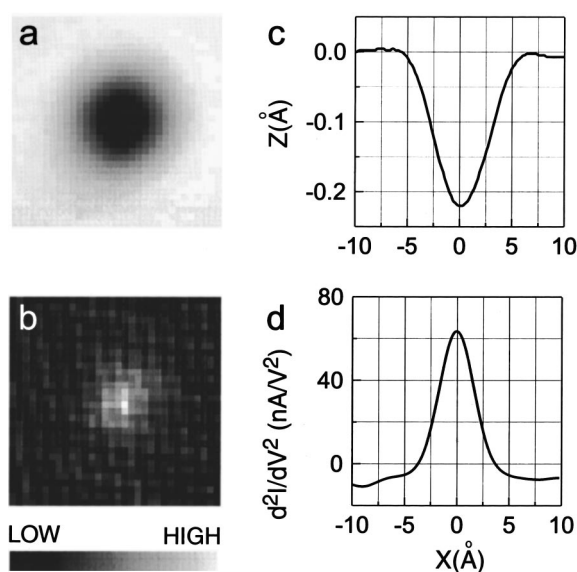


FIG. 2. Comparison of the CO constant current image and the spatial distribution of  $d^2I/dV^2$  at the hindered rotation energy for Cu(001). (a)  $14 \times 14$  Å constant current STM image taken at sample bias of 36 mV and a tunneling current of 1 nA. (b)  $d^2I/dV^2$  image taken concurrently. The raw data are shown with one pixel corresponding to one data point. The bias modulation amplitude was 7 mV. The image acquisition time was 7 min. (c) Cross section of (a) taken through the image minimum. (d) Cross section of (b) taken through the maximum of the smoothed image.

turned off and a 7 mV modulation at 200 Hz added to the bias. After a suitable number of time constants, the output of the lock-in measuring the second harmonic of the tunneling current was recorded to produce Fig. 2(b). Simultaneous vibrational and topographic imaging allows the lateral localization of the inelastic tunneling signal to be compared to the depression in the constant current image determined by the predominantly elastic tunneling current.

From Figs. 2(c) and 2(d), the FWHM of the CO topographic cross section is 6 Å compared to 4 Å for the vibrational image. Intrinsically, the width of the constant current image depends on the distance over which the electronic states responsible for tunneling contain significant character derived from the CO molecular energy levels.<sup>30</sup> The localization of the inelastic tunneling signal should depend on the localization of those electronic states which are coupled to the vibrational excitations of the molecule and vice versa. These electronic states may be a subset of the states sampled in the topographic image. In the present case of CO on copper, the vibrational peak is more localized than the constant current topographical depression.

This paper has demonstrated the ability of a stable, low-temperature STM to measure small conductance changes due to the vibrational excitation of a single CO molecule by inelastic electron tunneling. The detection of CO vibrational modes extends STM-IETS to a new functional group of a different nature than the C-H stretch previously observed.<sup>9</sup> The reported intensities of the tunneling-active C-O stretch and hindered rotation modes should assist in the development of a more complete theory of STM-IETS, which in turn will enhance the applicability of the technique. The spatial

localization of inelastic tunneling current is sufficient to allow vibrational microscopy to be performed with resolution comparable to conventional constant current images. STM-IETS may be applied to study the length scales on which steps, defects, and coadsorbates affect the vibrational spec-

trum of a single CO molecule. The strength of the technique lies in the ability to measure the vibrational spectrum and characterize the local environment of a single molecule.

This research was supported by the National Science Foundation under Grant No. DMR-9417866.

- 
- <sup>1</sup>*Vibrational Spectroscopy of Molecules on Surfaces*, edited by J. T. Yates, Jr. and T. E. Madey (Plenum, New York, 1987).
- <sup>2</sup>F. Hofmann and G. Toennies, *Chem. Rev.* **96**, 1307 (1996).
- <sup>3</sup>G. Binnig, N. Garcia, and H. Rohrer, *Phys. Rev. B* **32**, 1336 (1985).
- <sup>4</sup>D. P. E. Smith, M. D. Kirk, and C. F. Quate, *J. Chem. Phys.* **86**, 6034 (1987).
- <sup>5</sup>M. F. Crommie, C. P. Lutz, and D. M. Eigler, *Phys. Rev. B* **48**, 2851 (1993).
- <sup>6</sup>L. Ruan, F. Besenbacher, I. Stensgaard, and E. Laegsgaard, *Phys. Rev. Lett.* **70**, 4079 (1993).
- <sup>7</sup>J. Li, W.-D. Schneider, R. Berndt, and B. Delley, *Phys. Rev. Lett.* **80**, 2893 (1998).
- <sup>8</sup>V. Madhavan, W. Chen, T. Jamneala, M. F. Crommie, and N. S. Wingreen, *Science* **280**, 567 (1998).
- <sup>9</sup>B. C. Stipe, M. A. Rezaei, and W. Ho, *Science* **280**, 1732 (1998).
- <sup>10</sup>This estimate is based on the number of molecules required to achieve a signal-to-noise ratio of one under ideal conditions using macroscopic IETS. See R. M. Kroeker and P. K. Hansma, *Surf. Sci.* **67**, 362 (1977).
- <sup>11</sup>C. F. McConville, D. P. Woodruff, K. C. Prince, G. Paolucci, V. Chab, M. Surman, and A. M. Bradshaw, *Surf. Sci.* **166**, 221 (1986).
- <sup>12</sup>Ph. Hofman, K.-M. Schindler, S. Bao, V. Fritzsche, A. M. Bradshaw, and D. P. Woodruff, *Surf. Sci.* **337**, 169 (1995).
- <sup>13</sup>P. Uvdal, P.-A. Karlsson, C. Nyberg, S. Andersson, and N. V. Richardson, *Surf. Sci.* **202**, 167 (1988).
- <sup>14</sup>B. A. Sexton, *Chem. Phys. Lett.* **63**, 451 (1979).
- <sup>15</sup>C. J. Hirschmugl, G. P. Williams, F. M. Hoffmann, and Y. J. Chabal, *Phys. Rev. Lett.* **65**, 480 (1990); A. P. Graham, F. Hoffmann, J. P. Toennies, G. P. Williams, C. J. Hirschmugl, and J. Ellis, *J. Chem. Phys.* **108**, 7825 (1998).
- <sup>16</sup>J. Ellis, J. P. Toennies, and G. Witte, *J. Chem. Phys.* **102**, 5059 (1995).
- <sup>17</sup>J. Ahner, D. Mocuta, R. D. Ramsier, and J. T. Yates Jr., *Phys. Rev. Lett.* **79**, 1889 (1997).
- <sup>18</sup>B. Voigtländer, D. Bruchmann, S. Lehwald, and H. Ibach, *Surf. Sci.* **225**, 151 (1990).
- <sup>19</sup>H. Kato, M. Kawai, and J. Yoshinobu, *Phys. Rev. Lett.* **82**, 1899 (1999).
- <sup>20</sup>B. C. Stipe, M. A. Rezaei, and W. Ho, *Rev. Sci. Instrum.* **70**, 137 (1999).
- <sup>21</sup>In all measurements, the root-mean-square (rms) value of the modulation is reported.
- <sup>22</sup>R. M. Kroeker, W. C. Kaska, and P. K. Hansma, *J. Chem. Phys.* **74**, 732 (1981).
- <sup>23</sup>P. S. Bagus, C. J. Nelin, W. Müller, M. R. Philpott, and H. Seki, *Phys. Rev. Lett.* **58**, 559 (1987).
- <sup>24</sup>M. Head-Gordon and J. C. Tully, *Chem. Phys.* **175**, 37 (1993).
- <sup>25</sup>B. N. J. Persson and J. E. Demuth, *Solid State Commun.* **57**, 769 (1986).
- <sup>26</sup>B. N. J. Persson and A. Baratoff, *Phys. Rev. Lett.* **59**, 339 (1987).
- <sup>27</sup>M. A. Gata and P. R. Antoniewicz, *Phys. Rev. B* **47**, 13 797 (1993).
- <sup>28</sup>For positive (negative) bias the electrons tunnel from the tip (adsorbate-substrate) to the adsorbate-substrate (tip). See, e.g., *Tunneling Spectroscopy*, edited by P. K. Hansma (Plenum, New York, 1982).
- <sup>29</sup>L. J. Lauhon and W. Ho (unpublished).
- <sup>30</sup>The CO corrugation also depends on the gap resistance and the tip sharpness.
- <sup>31</sup>D. P. Woodruff, B. E. Hayden, K. Prince, and A. M. Bradshaw, *Surf. Sci.* **123**, 397 (1982).